Monolithically prepared aqueous supercapacitors

Jari Keskinen, Anna Railanmaa, Donald Lupo*

Tampere University of Technology, Laboratory of Electronics and Communications Engineering, Korkeakoulunkatu 3, FI-33720 Tampere, Finland

e-mail jari.keskinen@tut.fi

telephone +358 3 311511

Keywords: supercapacitor, printed electronics, aqueous electrolyte, electrode, energy storage, chitosan

Highlights:

- Aqueous supercapacitors fabricated by applying solutions on top of each other
- Inexpensive and simple manufacturing method
- Environmentally friendly non-toxic materials
- Biopolymer chitosan used as electrode binder and separator

Abstract

We demonstrate a novel method to manufacture non-toxic supercapacitors with aqueous electrolyte by solution processing techniques. The supercapacitors are fabricated on flexible substrates by applying ink layers on top of each other resulting to a monolithic structure. In this

way the whole component including current collectors, electrodes and separator can be implemented on one substrate without the need to align and seal two separately fabricated electrodes. Biopolymer chitosan has an important role since it acts both as separator and activated carbon electrode binder. This work facilitates an easier manufacturing of thin supercapacitor structures e.g. for Internet of Things (IoT) and sensor network applications. The capacitance range of our components is 0.26-0.43 F and equivalent series resistance 12-32 Ω.

1. Introduction

Electrochemical supercapacitors[1,2] are energy storage devices having high specific power, wide temperature range and long lifetime. An electrochemical supercapacitor has two electrodes separated by an ionically conductive electrolyte. In practical supercapacitors the electrodes are porous and filled with the electrolyte. To prevent a short-circuit between the electrodes, a porous separator is usually installed between the electrodes. The pores allow movement of ions, while the solid structure prevents a short circuit between the two electrodes. The electrodes are typically made of activated carbon (AC) powder with a binder material[3] that can be a fluorine containing polymer such as PTFE or PVDF or e.g. a biopolymer like cellulose. The alternatives for electrolytes include organic or water based solvents with dissolved ions or ionic liquids[4].

Sensor networks and Internet of Things (IoT) devices would benefit from small inexpensive energy storage components[5] that do not contain toxic materials and can thus be recycled or incinerated with normal household waste. The primary or secondary batteries currently used for these applications typically contain metals such as lithium, silver or manganese and are encapsulated inside a metal package. Battery electrodes may also be corrosive in case a leakage takes place, and

some batteries contain harmful organic solvents. Using primary batteries often results to the need to replace the batteries periodically. In applications where long lifetime is needed, the cycle life of secondary batteries may not be long enough thus making the battery change necessary. Supercapacitors, together with an energy harvesting device such as e.g. photovoltaic cell or piezoelectric generator, can solve these shortcomings since they have long lifetime and they can be made of inexpensive non-toxic raw materials using mass production methods such as printing.[6,7,8,9] If the application requires high peak power, supercapacitors can be used in parallel with a low-power energy source to meet the demands.[10]

Printed energy storage devices are typically manufactured by fabricating the electrodes separately followed by an assembly step where a separator is placed between the electrodes, electrolyte is added and the package is sealed. This method is called stacked assembly.[8,11] The aim of this work is to provide a novel manufacturing process concept that makes the fabrication of supercapacitors easier by eliminating the assembling step requiring aligning and sealing of separate electrodes and separator. The result is a monolithic structure consisting of substrate, two electrodes, two current collectors and separator.

It is also possible to avoid the alignment and assembly step by using interdigitated electrodes in the substrate plane instead of arranging them vertically.[12,13] However, the interdigitated structure leads to high equivalent series resistance (ESR) due to the long current collectors. To achieve reasonably low ESR, we prefer the geometry of stacked assembly in which the electrodes are face-to-face.

The use of environmentally benign materials in energy storage devices is beneficial.[14] The materials chosen in this work are non-toxic, facilitating the use of the supercapacitors even in disposable applications. We present a process in which the layers of a supercapacitor are coated on top of each other using solutions as raw materials. The separator is made of chitosan solution and it is also used as binder in electrodes. Chitosan is prepared from chitin, the second most abundant natural polymer in the world. It is non-toxic, biodegradable, and biocompatible.[15] Examples of suitable applications for our supercapacitors include energy autonomous systems together with, for example, piezoelectric or RF harvester.[16,17]

2. Experimental

The materials choice of the supercapacitor was largely defined by the requirement that the total system should be non-toxic, recyclable and incineratable. In addition, the need to print the parts on top of each other required compatibility of the materials with respect toadhesion and wettability. The current collectors and active material layers were made of printing inks, avoiding the use of fluorine-containing binders. The electrolyte was an aqueous, non-toxic salt solution.

PET foil (Melinex ST506 from DuPont Teijin Films, thickness 125 µm) and PET/aluminium laminate (Walki, thicknesses of the layers 50 and 9 µm, respectively) were used as substrates. In the case of PET/Al laminate, the supercapacitor structure was on the PET side and thus the aluminium layer acted only as barrier layer. The current collectors were made of Acheson PF407C graphite ink. The ink curing temperature was chosen to be 95 ^{o}C. The raw materials for the electrode ink were Kuraray YP-80F activated carbon, chitosan (Sigma-Aldrich Chitosan from

shrimp shells, 50494), acetic acid and deionized water (mass percentages 25.8, 1.4, 0.6 and 72.2, respectively).

The cross-section and layout of the manufactured supercapacitors are shown in figures 1 a and b. Both the width and the length of the supercapacitor are 50 mm and the total thickness 0.5-0.8 mm. The manufacturing process of the layer-by-layer fabricated supercapacitors starts by applying the lower graphite ink to act as current collector (red in the figure 1a, width 34 mm). On top of that activated carbon (larger black rectangle) layer (32 mm x 10 mm) is applied. The next layer is the separator (blue, 26 mm x 16 mm). In one of the layer-by-layer fabricated supercapacitor types (A) we used 40 µm thick Dreamweaver Silver AR40 cellulose paper as separator to compare the properties of chitosan and paper separators. In other types (B-E) the separator materials used were chitosan (Sigma-Aldrich 50494) as such and with talc (Finntalc M15E) as filler material. On top of the separator the upper electrode (black, 24 mm x 10 mm) and the upper current collector is applied (green, width 18 mm). When these layers are ready, the electrolyte is added. The alternatives for encapsulation (yellow) have been the same materials used as substrate or epoxy (Loctite Power Epoxy Universal) to make the supercapacitor completely solution processable. The foils used as top encapsulation were heat-sealed using Paramelt Aquaseal X2277 polyolefin dispersion.

The manufacturing process of the reference supercapacitors (F) is partly similar to the one used with layer-by-layer fabricated supercapacitors and is described in detail in the article by Keskinen et al.[8] Two current collectors are made (graphite ink, red and green in the figure 1b) and AC ink layers applied on them. The same Dreamweaver separator is assembled between the electrodes,

the electrodes and separator are impregnated with electrolyte and the whole system is heat-sealed with Paramelt Aquaseal X2277 (gray).

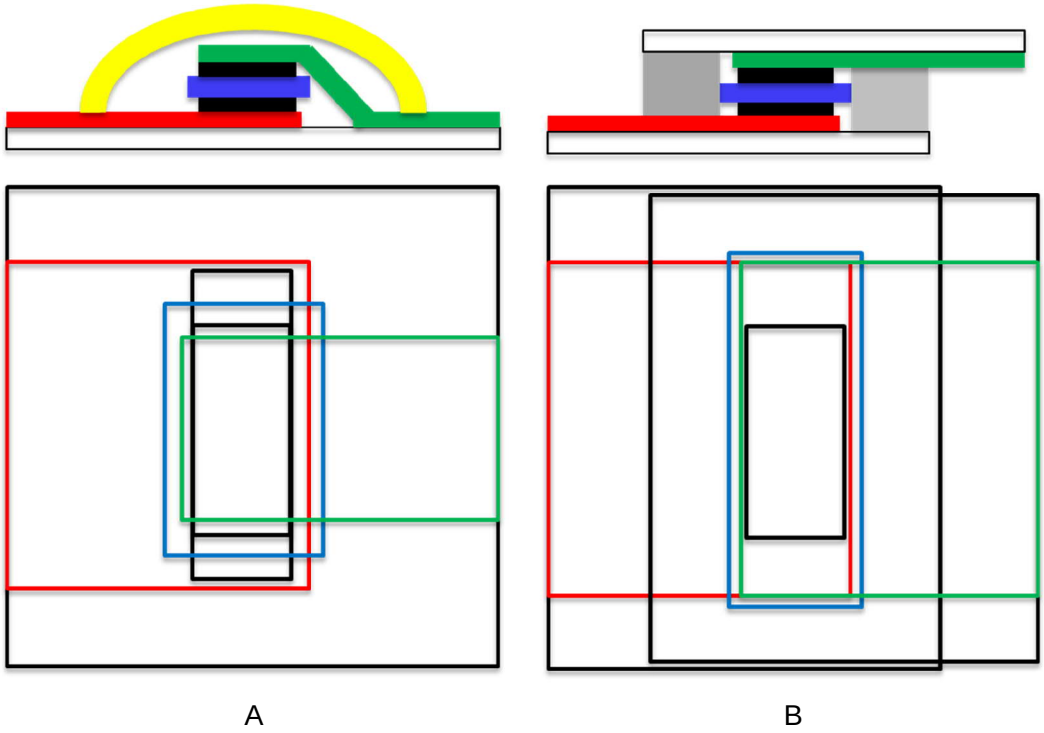

Figure 1. Schematic cross-sections and layouts of the layer-by-layer fabricated supercapacitor (a) and the conventional supercapacitor (b) used as reference. The vertical and horizontal dimensions in the cross-section figures are not in the same scale.

There are several requirements for the separator layer. Obviously, it must be ionically conductive to facilitate the electrical operation of the supercapacitor. It also needs to guarantee the electrical insulation between the electrodes to prevent short circuits. In addition, it has to be compatible with

the graphite and activated carbon inks first by adhering on them and secondly allow the application of the upper activated carbon and graphite ink layers.

A laboratory scale doctor blade coater (mtv messtechnik) was used for applying the current collector and AC inks. The AC ink was dried at room temperature resulting in films with thickness of 70-100 µm. Stencils were used to define the lateral dimensions of the current collectors, electrodes and chitosan separators. The registration accuracy in the plane of the substrate is limited in our case by the manual alignment of the stencil and is in practice of the order of 0.5 mm. The wet thickness of the current collectors and the electrodes was 100 µm and defined by the stencil. After drying the total mass of the two electrodes was 10-20 mg. The wet thickness of the chitosan solution layer was 1 mm and defined by the height of the doctor blade. The screen printing of the graphite and activated carbon inks has been demonstated earlier.[9]

The electrolyte was made by diluting pro analysis grade NaCl to deionized water in mass ratio 1:5. The electrolyte was applied using a pipette just before encapsulating the device. The penetration of the electrolytes inside the electrodes is clearly visible and since the bottom electrode is larger than the separator and the upper electrodes is smaller than the separator, it is possible to observe the wetting when electrolyte is dropped to one edge of the electrode. We let the electrolyte penetrate inside the electrodes and separator before the encapsulation process.

Table 1 shows the structural and material differences between the manufactured supercapacitors.

Sample	Substrate	Separator	Cap	Structure

A	PET/Al	2-fold paper	PET/Al	Layer-by-layer
B	PET	Chitosan	PET	Layer-by-layer
C	PET/Al	Chitosan	PET/Al	Layer-by-layer
D	PET/Al	Chitosan+talc	PET/Al	Layer-by-layer
E	PET/Al	Chitosan	Epoxy	Layer-by-layer
F (reference)	PET/Al	Paper	NA	Face-to-face assembled

Table 1. Supercapacitor materials and structures.

The cross-section micrographs of the supercapacitor structures were examined with scanning electron microscope (SEM) Zeiss Supra 55.The samples were prepared in two different ways: by casting the supercapacitor structure inside epoxy and then grinding with SiC paper or by broad ion beam (BIB) method using a Gatan Ilion^{TM} device.

The electrical properties of the capacitors such as capacitance, equivalent series resistance (ESR), and leakage current were determined according to the IEC 62391-1 standard[18] using a Maccor 4300 instrument. The cyclic voltammetry (CV) measurements were performed with the same instrument, but not used for defining numerical values, only to illustrate the behaviour of the supercapacitors. In the measurement procedure, the component was first charged and discharged with constant current (1, 3 and 10 mA) between 0 and 1.2 V three times, then the voltage was kept for 30 minutes at 1.2 V, after which the capacitance was defined during the constant current discharge step between 0.96 V and 0.48 V potential. After keeping the supercapacitor for 1 hour at constant voltage, the current required to maintain the potential was measured to get the leakage current value. The efficiency was defined as the ratio of the discharged and charged energy in the voltage range of 0 -1.2 V. The ionic resistance of chitosan film was determined with impedance

spectroscopy using a Zahner Zennium potentiostat potentiostat and the resistance of the activated carbon electrode using four-point measurement.

3. Results and discussion

3.1. Manufacturing process development

Supercapacitors with various materials and structures are here compared with each other and the reference. Photos of of the supercapacitor architectures reported here are shown in Figure 2. The external appearance of the supercapacitors of type A, C and D is similar to each other. The main difference in the appearance in type B is that due to the transparency of the PET substrate and cap the current collector structure is clearly visible. The epoxy cap is clearly visible in component type E. Thus in component E all layers are fabricated using solution processing. Due to the face-to-face configuration of the contact surfaces of the supercapacitor F, the negative and positive contacts are located on the opposite sides.

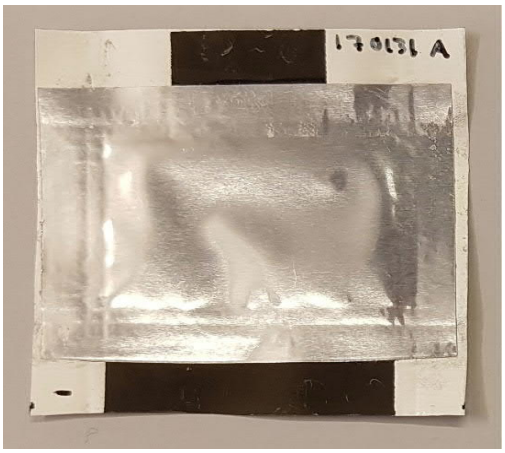

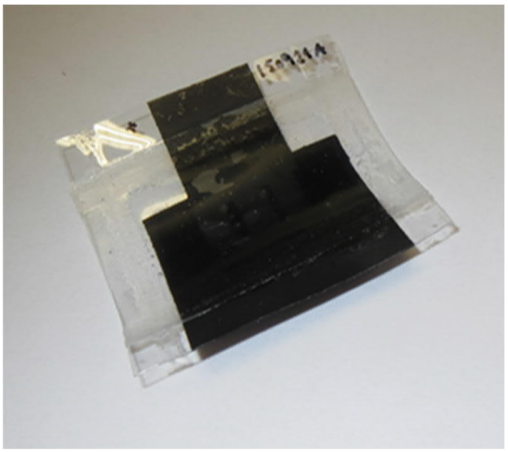

A, C, D

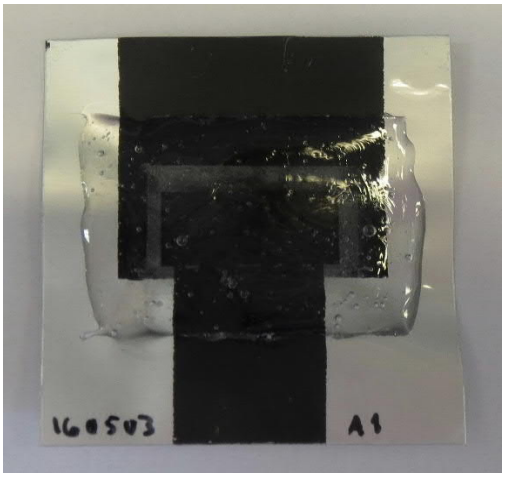

B

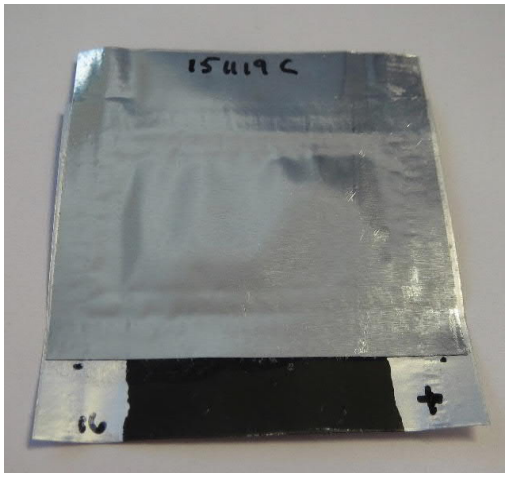

E

F

Figure 2. Appearances of the fabricated supercapacitor types.

The starting point for the research work was the supercapacitor of type F, which is here used as a reference. In the following, the effect of the fabrication parameters of the layer-by-layer fabricated supercapacitors on the most essential properties is reviewed.

Type A was a prototype to test the concept of layer-to-layer manufacturing method still using paper separator. To prevent the penetration of the upper AC ink through the separator, two-fold paper was used. In type B the structure including chitosan separator was applied on PET substrate and the same structure was repeated in type C on PET/Al to benefit from the barrier properties of aluminium. Due to the shrinkage of chitosan during curing, in type D talc was added to chitosan separator solution to decrease dimensional changes during the drying. Type E is the structure where all layers are made of solutions and thus the concept of making the whole supercapacitor using solution processing,thus potentially by printing, was realized.

3.2 Microstructure

Figure 3a shows the microstructure of the cross-section of a complete supercapacitor. The PET layer of the substrate is on the left and is bright due to charging in the SEM. The thicknesses of the layers are approximately the following: bottom graphite ink current collector 20 µm, lower AC electrode 70 µm, chitosan with talc binder separator 20 µm, upper electrode 100 µm and top current collector 15 µm. Although the upper electrode and current collector were intended to be identical compared to the lower ones, thicker layers were obtained since the doctor blade method led to larger wet thicknesses due to the warping of the supercapacitor structure.

Figure 3b is taken with higher magnification and reveals the microstructure of the electrodes more clearly, showing activated carbon particles of up to about 10 µm in size.

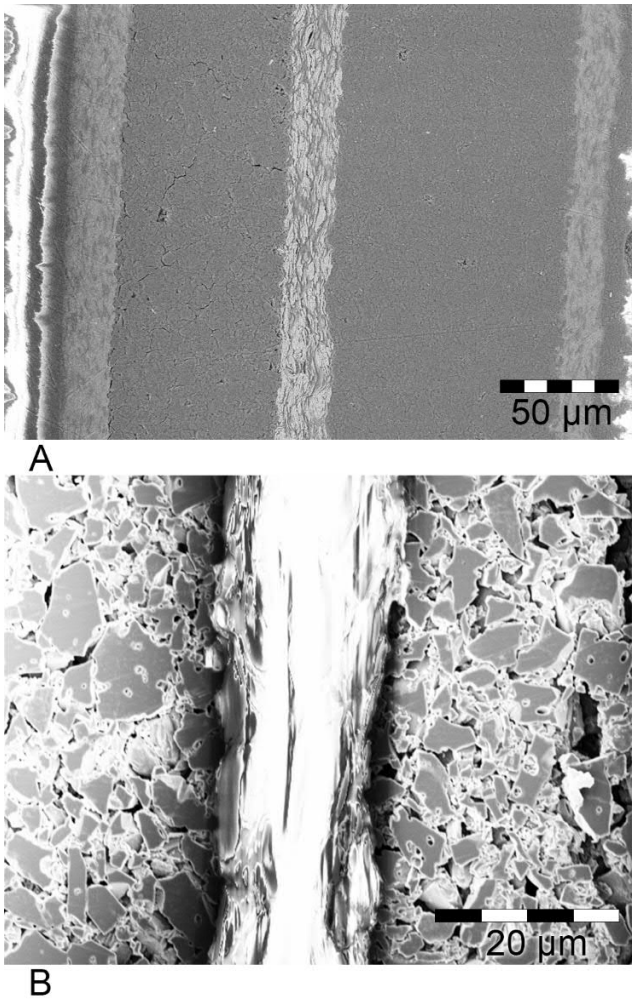

Figure 3. Cross-section of the supercapacitor (a) and microstructure of the electrodes around the separator (b). (a) is from a grinded and (b) from a broad-ion-beam processed sample.

3.3 Electrical properties

Figure 4 shows constant current charge/discharge behaviour with two current values and the cyclic voltammetry curves measured with three different scan rates. The ideal CV loop shape for a capacitor is a rectangle. In practice, equivalent series resistance (ESR) flattens the rectangle.[19] Table 2 contains the electrical values measured as described in the experimental part of this paper.

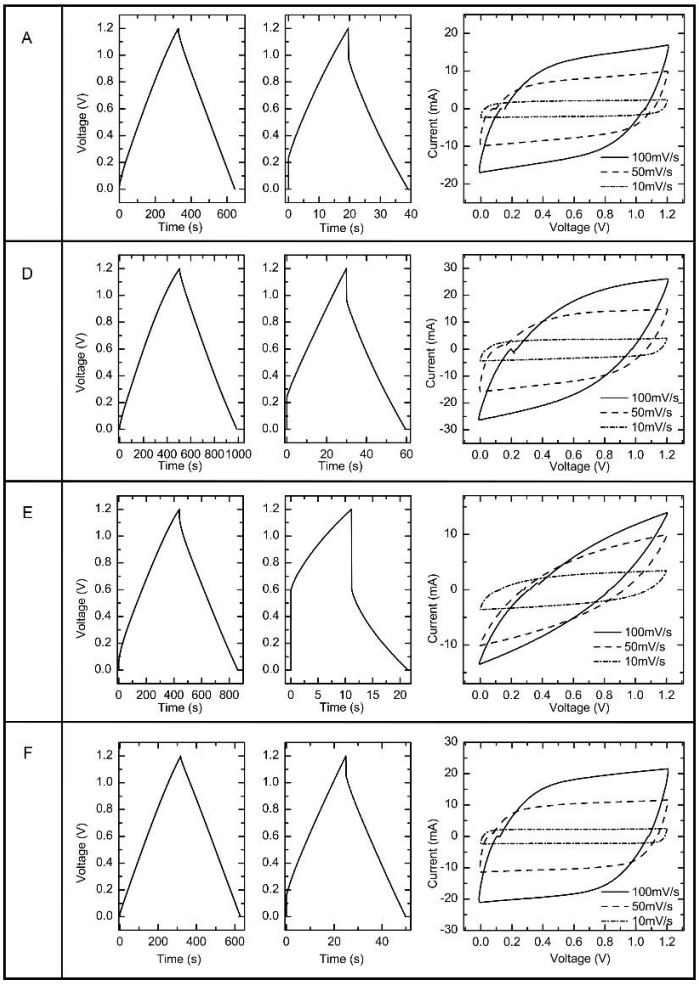

Figure 4. Galvanostatic (1 mA and 10 mA) and cyclic voltammetry measurements for the supercapacitors A, D, E and F. In the CV curves the steps when changing the current direction are due to the measurement device.

Type	Capacitance (F)	ESR (Ω)	Leakage current (µA)	Leakage to capacitance ratio (μAF^{-1})	Energy efficiency (%)
A	0.29	12	7.9	27	81
B	0.26	30	27	104	62
C	0.32	15	13	41	71
D	0.43	12	13	30	75
E	0.41	32	16	39	71
F (reference)	0.27	8.3	5.7	21	90

Table 2. Electrical properties

The capacitance values are relatively near to each other, ranging between 0.26 and 0.43 F. The variations are largely due to the lack of repeatability of electrode thickness due to the warping of the substrate because of chitosan separator shrinkage and its effect on the doctor blade coating. The area of the positive and negative electrodes was not the same, in order to avoid short circuit when applying the electrode and current collector layers and to leave the edges of electrodes bare in order to facilitate electrolyte penetration inside the porous electrodes. Because of the smaller upper electrode, in practice the edges of the lower electrode do not effectively participate in charging and discharging the supercapacitor. The same activated carbon ink has demonstrated specific capacitance of 26-29 Fg^{-1} (corresponds to 104-116 Fg^{-1} for single electrode) in earlier experiments.[8]

The maximum energy stored in a supercapacitor is given by [20]

$$W = \frac{1}{2}CU^2 \qquad (1)$$

Where *C* is the capacitance and *U* is the maximum potential across the supercapacitor. For a 0.4 F supercapacitor having 1.2 V potential the stored energy is thus 0.288 J. The geometrical area of the electrode is 3.2 cm^2 and the total volume and mass of two electrodes and a separator 0.064 cm^3 and about 20 mg, respectively. From these figures the specific capacitance relative to the mass and area of the electrodes are 20 F/g and 0.13 F/cm^2 and specific capacitance relative to electrode and separator volume 6.3 F/cm^3. The corresponding energy density values are 44 J/g, 90 mJ/cm^2 (=25 $\mu Wh/cm^2$) and 4.5 J/cm^3 (=1.2 mWh/cm^3). When compared with values given in recently published review articles dealing with microsupercapacitors [21, 22], our energy per area values are clearly above median.

The ESR of the supercapacitor consists of the Ohmic resistance due to the current collectors and activated carbon layer and the ionic resistance in the electrolyte. In addition, there is also contact resistance between the layers. As is the case of capacitance values due to electrode thickness variations, the ESR values are also affected by different graphite ink layer thicknesses. The square resistance of the graphite ink has been specified by the ink manufacturer specification to be below 20 Ω/sq for a 25 µm thick layer. The manufacturer also reports the square resistance for each batch and they have been about 11-14 Ω/sq. Since the thickness of the cured current collector ink is typically 20-30 µm, taken the geometry of the current collector into account results to total resistance of two current collectors to be of the order of 10-30 Ω. The resistivity of the cured activated carbon electrode ink is 0.70 Ωm. Using this value together with the dimensions of the electrodes (area 2.4 cm^2 and thickness 100 µm), the resistance of each electrode is 0.29 Ω. The ionic resistance of the chitosan film soaked with electrolyte is 0.8 Ωm. The chitosan layer swells when soaked which was taken into account when the ionic resistance of the chitosan layer was

calculated. As dry thickness we used 20 µm (Figure 3A) and area 2.4 cm^2. Then the contribution of chitosan separator to the ESR would be 0.17 Ω. Thus the majority of the ESR in supercapacitors is due to the graphite current collectors. In the figure 4, when comparing the CV and galvanostatic curves, the tilted CV curve clearly correlates with higher IR drop. The lower ESR of the reference sample type F partly originates from the difference in current collector width: in the layer-by-layer fabricated type the upper current collector is narrower.

The maximum usable power of a supercapacitor can be calculated according to [20]

$$P = \frac{U^2}{4R} \quad (2)$$

Where R is the total ESR. Thus e.g. for R = 12 Ω and U = 1.2 V, the maximum power would be 30 mW. With the same dimensions and masses used above to calculate specific energy, the specific power values are 1.5 W/g, 9.4 mW/cm^2 and 0.47 W/cm^3. Obviously, for the highest ESR of 32 Ω these values should be multiplied by 0.375. When compared with the values published by other groups for microsupercapacitors[21, 22], these are below average. To decrease ESR, it would be possible to use thicker graphite ink current collectors or further optimize the layout to shorten the distance from the activated carbon electrode to the contact outside the supercapacitor. The ESR could be reduced considerably by introducing current collectors with metal foil or e.g. silver ink.[7,8] However, using metal current collectors would increase the corrosion risk with aqueous electrolytes[8], and is thus not preferred if the application does not require lower ESR.

Leakage current is believed to result primarily from impurities participating in Faradaic charge-transfer reactions at the electrodes.[8] The impurities may originate from carbon materials or chitosan. Oxygen dissolved in the electrolyte and adsorbed on the surface of the activated carbon

also increases leakage current.[1] The supercapacitors were assembled in ambient air, and thus oxygen is present in the electrolyte.

Since there is a correlation between the leakage current and capacitance,[8] table 2 also includes the ratio between these. This ratio is a more functional measure to compare supercapacitors than leakage current alone. The leakage current is lowest in the reference and sample A, which essentially have similar materials. The supercapacitors with chitosan separator have somewhat higher leakage current, which may be due to impurities in chitosan. The highest leakage current was obtained for the component of type B, which in addition to chitosan separator as a potential cause for increased leakage current, does not have an aluminium barrier. Thus also oxygen from air penetrating to the electrolyte may contribute to the increased leakage current.[8]

Both ESR and leakage current contribute to the energy efficiency of a supercapacitor. The energy efficiencies in Table 2 were defined for all components with 1 mA charge and discharge current. Clearly the reference component, having the lowest ESR and leakage current, also shows the highest energy efficiency. Of the solution processed supercapacitor structures, from the starting point of type B, the energy efficiency was improved in types C, D and E by having lower ESR and leakage current.

The electrical properties of the layer-by-layer fabricated supercapacitors can be considered to be adequate for the IoT applications including the necessary communications and sensor functions[23, 24, 25]. Using the chitosan separator is a feasible alternative to commonly used paper separators although it increases the leakage current. Depending on the application, the higher

leakage current can be compensated by charging the supercapacitor more often or by increasing the capacitance. For all the manufactured component types, an output current of 1 mA is feasible. While this current is not sufficient for high peak power radio transmission such as Bluetooth, it is above peak power expected for energy efficient wireless sensor nodes, as described in the references cited above.

4. Conclusions

Different layer-by-layer fabricated monolithic supercapacitor structures were prepared by solution processing. The design was guided by the demand of non-toxic materials and easy manufacturing method using printing methods. Chitosan acted both as activated carbon binder and ionically conducting separator. The capacitance of the manufactured supercapacitors was 0.26 – 0.43 F. The ESR values of the layer-by-layer fabricated supercapacitors varied from 12 to 32 Ω, and the majority of ESR was due to using graphite ink current collectors.

Although fabricating the supercapacitors layer-by-layer caused the electrical properties such as ESR and leakage current to be inferior to those obtained for a conventional structure, it was found feasible to use the design when it is advantageous to be able to manufacture supercapacitors without the need of separate assembling step to align the electrodes and simultaneously fill in the electrolyte.

Funding

Financing from Tekes – the Finnish Funding Agency for Innovation including decisions 40146/14 and 40337/14 is gratefully acknowledged.

References

[1] B.E. Conway, Electrochemical Supercapacitors: Scientific Fundamentals and Technological Applications, Springer US, Boston, 1999.

[2] F. Béguin, E. Frackowiak, Supercapacitors: Materials, Systems and Applications, Wiley-VCH, Weinheim, Germany, 2013.

[3] Z. Zhu, S. Tang, J. Yuan, X. Qin, Y. Deng, R. Qu, G.M. Haarberg, Effects of Various Binders on Supercapacitor Performances. Int. J. Electrochem. Sci., 11 (2016) 8270 – 8279.

[4] C. Zhong, Y. Deng, W. Hu, D. Sun, X. Han, J. Qiao, J. Zhang, Electrolytes for Electrochemical Supercapacitors, CRC Press, Boca Raton, USA, 2016.

[5] A. Somov, R. Giaffreda, Powering IoT Devices: Technologies and Opportunities, IEEE Internet of Things Newsletter, November 2015, https://iot.ieee.org/newsletter/november-2015/powering-iot-devices-technologies-and-opportunities.html (accessed 18.08.30)

[6] H. Zhang, Y. Qiao, Z. Lu, Fully Printed Ultraflexible Supercapacitor Supported by a Single-Textile Substrate, ACS Appl. Mater. Interfaces 8 (2016) 32317−32323.

[7] J. Keskinen, E. Sivonen, S. Jussila, M. Bergelin, M. Johansson, A. Vaari, M. Smolander, Printed supercapacitors on paperboard substrate, Electrochim. Acta 85 (2012) 302–306.

[8] J. Keskinen, S. Lehtimäki, A. Dastpak, S. Tuukkanen, T. Flyktman, T. Kraft, A. Railanmaa, D. Lupo, Architectural Modifications for Flexible Supercapacitor Performance Optimization. Electron. Mater. Lett. 12 (2016) 795-803.

[9] S. Lehtimäki, A. Railanmaa, J. Keskinen, M. Kujala, S. Tuukkanen, D. Lupo, Performance, stability and operation voltage optimization of screen-printed aqueous supercapacitors, Sci. Rep. 7:46001 (2017) 1-9.

[10] J. Keskinen, E. Sivonen, M. Bergelin, J.-E- Eriksson, P. Sjöberg-Eerola, M. Valkiainen, M. Smolander, A. Vaari, J. Uotila, H. Boer, S. Tuurala, Printed supercapacitor as hybrid device with an enzymatic power source. Adv. Sci. Tech. 72 (2010) 331-336.

[11] S. Tuukkanen, M. Krebs, Printable Power Storage: Batteries and Supercapacitors, in: G. Nisato, D. Lupo, S. Ganz, (Eds.), Organic and Printed Electronics, Pan Stanford Publishing: Boca Raton, USA, 2016, pp. 265-291.

[12] R. Kumar, R. Savu, E. Joanni, A.R. Vaz, M.A. Canesqui, R.K. Singh, R.A. Timm, L.T. Kubota, S.A. Moshkalev, Fabrication of interdigitated micro-supercapacitor devices by direct laser writing onto ultra-thin, flexible and free-standing graphite oxide films, RSC Adv. 6 (2016) 84769-84776.

[13] J. Li, V. Mishukova, M. Östling, All-solid-state micro-supercapacitors based on inkjet printed graphene electrodes. Appl. Phys. Lett. 109 (2016) 123901-1 – 123901-4.

[14] B. Dyatkin, V. Presser, M. Heon, M.R. Lukatskaya, M. Beidaghi, Y. Gogotsi, Development of a Green Supercapacitor Composed Entirely of Environmentally Friendly Materials. ChemSusChem 6 (2013) 2269–2280.

[15] H. Honarkar, M. Barikani, Applications of biopolymers I: chitosan, Monatsh Chem 140 (2009) 1403–1420.

[16] J. Pörhönen, S. Rajala, S. Lehtimäki, S. Tuukkanen, Flexible Piezoelectric Energy Harvesting Circuit With Printable Supercapacitor and Diodes, IEEE Trans. Electron Devices 61 (2014) 3303-3308.

[17] S. Lehtimäki, M. Li, J. Salomaa, J. Pörhönen, A. Kalanti, S. Tuukkanen, P. Heljo, K. Halonen, D. Lupo, Performance of printable supercapacitors in an RF energy harvesting circuit. Int. J. Electr. Power Energy Syst. 58 (2014) 42-46.

[18] Standard IEC 62391-1. Fixed electric double-layer capacitors for use in electronic equipment, 2006.

[19] B. Shia, Materials Synthesis and Characterization for Micro-supercapacitor Applications. Ph.D. Thesis, University of California, Berkeley, USA, 2013.

[20] R. Kötz, M. Carlen, Principles and applications of electrochemical capacitors, Electrochim. Acta 45 (2000) 2483-2498.

[21] N. Kyerematen, T. Brousse, D. Pech, Microsupercapacitors as miniaturized energy storage components for on-chip electronics, Nat. Nanotech. 12 (2017) 7-15.

[22] C. Chen, S. Xu, Y. Xie, M. Sanghadasa, X. Wang, A Review of On-Chip Micro Supercapacitors for Integrated Self-Powering Systems, J. Microelectromech. Syst. 26 (2017) 949-965.

[23] J. Rinne, J. Keskinen, P. Berger, D. Lupo, M. Valkama, Feasibility and Fundamental Limits of Energy-Harvesting bases M2M Communications, Int. J Wireless Information Networks, 2017, DOI 10.1007/s10776-017-0358-z.

[24] T. Haapala, M. Pulkkinen, J. Salomaa, K. Halonen, A 180-nW Static Power UWB IR Transmitter Front-End for Energy Harvesting Applications, Proc. IEEE International Symposium on Circuits and Systems (ISCAS), Baltimore, MD, USA, May 28 – 31, 2017.

[25] J. Salomaa, S. Jamali-Zavareh, M. Pulkkinen, S. S. Chouhan, K. Halonen, Ultra-Low Power Incremental Delta-Sigma ADC for Energy Harvesting Sensor Applications, Analog Integr Circuits Signal Process., 92 (2017) 369-382.